Electrostatic Fluid Accelerator and Air Purifier – The Second Wind

I.A. Krichtafovitch[1], V.L. Gorobets[1], S.V. Karpov[1], and A.V. Mamishev[2]

[1]Kronos Air Technologies
8551 154th Ave NE
Redmond, WA 98052
phone: (425) 885-9739
email: ik@kronosati.com

[2]Department of Electrical Engineering
University of Washington
Seattle WA 98125

***Abstract*—Transformation of ionic pump (electron wind, Electrostatic Fluid Accelerator) technology from curious laboratory experiments to practical industrially acceptable devices requires pushing the basic technology to its physical limits. This paper presents a description of main design optimization options. A numerical modeling study demonstrates the effect of geometry and voltage distribution on the performance of the single stage of an Electrostatic Fluid Accelerator. The theoretical model comprises coupled quasielectrostatics and fluid dynamics. Experimental data obtained with multi-stage accelerators demonstrates that high air velocities can be achieved using this approach.**

I. INTRODUCTION

Electrostatic air pumps, also known as ionic wind pumps, have been examined for use in such applications as air propulsion [1-3], solid-fluid boundary layer modification [4,5], cooling [6-13], electro-acoustics [14], particulate removal [15], and dehumidification [16,17]. The efficiency and air velocities achieved in the earlier prototypes of ionic wind pumps remained so low that it prevented their widespread use. For decades, the practical industrial applications of corona-based devices were limited mostly to electrostatic precipitators. Recent research efforts, however, indicate that optimization of design of ionic pumps may lead to great improvements of their operational characteris-

tics, and, eventually, to their widespread use. The results of presented study are applicable primarily to the design of air pumps, dubbed here as Electrostatic Fluid Accelerators (EFA) as an alternative to traditional rotary fans.

The classical rotary structural geometry, although used in numerous applications, is limited in both scale and design flexibility, due to the necessity of high-speed rotating parts. Turbulent flow, vibration, and gyroscopic forces introduce inherent inefficiency and noise to a rotary system. Even in the applications for which noise and vibrations do not present a significant problem, rotary fans are difficult to optimize for more than a single air flow circulation pattern, due to their nearly static cross-sectional air velocity profile. Ionic wind pumps offer nearly laminar air propulsion with dynamic airflow profiles, controllable air velocities, and a possibility to decrease the effective boundary layer at the solid-fluid interface [18,19]. In addition, ionic propulsion is achieved without moving mechanical parts, thus enabling flexible design and possible integration at the MEMS level [10,20].

An overwhelming majority of the existing electrostatic air propulsion devices have simple electrode geometry, convenient for theoretical modeling, but are sub-optimal in terms of air velocity, backpressure, efficiency, and longevity [21-25]. This paper focuses on methods used to improve the design of multi-electrode EFAs through the changes of geometry and electrical excitation patterns. The multi-physics theoretical modeling proves invaluable in the analysis of effects of different design approaches. The modeling approach is discussed in context of a representative problem: movement of air molecules in narrow channels. Experimental data presented at the end of this paper shows that the described approach leads to EFA designs with very high air velocities.

II. Design considerations

The velocity of the air at the outlet of EFA is limited by three main factors: 1) the size of the device, 2) the energy density released in the volume of the device, and 3) the efficiency of conversion of input electrical energy into the kinetic energy of the moving air. Each of these factors suggests a possible class of improvements to the canonical needle-to-plane and wire-to-rod geometries of ionic pumps. Each factor is discussed separately next.

A. Device size

One way to increase the air velocity at the outlet of the EFA is to stack several corona-collector pairs in the direction parallel to the air stream [26]. A straight-forward stacking of several devices leads to several undesired side effects, and, ultimately, inability to achieve theoretical optimal performance.

One of these side effects is excessive size requirements for multi-stage EFA devices, since several stages of EFAs, placed in succession, require a substan-

tial length along an air duct (i.e., along air flow direction). This lengthy duct further presents greater resistance to air flow.

When stages are placed close to each other, the reduced spacing between the stages may produce a strong electric field between an attractor (or collecting) electrode of one stage and a corona discharge electrode of an adjacent next stage. This electric field may induce corona that will result in a reversed air flow. Moreover, due to the electrical capacitance between the neighboring stages, there is a parasitic current flow between them. This current is caused by non-synchronous high voltage ripples or high voltage pulses between neighboring stages.

Yet another problem with multiple stage designs is that each separate (or groups of) stage(s) is equipped with its own high voltage power supply (HVPS). In this case, the high voltage required to create the corona discharge may lead to an unacceptable level of sparks generated between the electrodes. When a spark is generated, the HVPS must completely shut down for some period of time required for deionization and spark quenching prior to resuming its operation. As the number of electrodes increases, sparks are generated more frequently than with one set of electrodes. If one HVPS feeds several sets of electrodes (i.e., several stages), then it is necessary to shut down more frequently to extinguish the increased number of sparks generated. That leads to an undesirable increase in power interruption for the system as a whole. To address this problem, it may be beneficial to feed each stage from its own dedicated HVPS. However, using separate HVPS requires that consecutive stages be more widely spaced to avoid undesirable electrical interactions caused by stray capacitance between the electrodes of neighboring stages and to avoid production of a back corona.

The EFA designs used for experiments discussed later in this paper employ innovative solutions to increase airflow by closely spacing EFA stages while minimizing or avoiding the introduction of undesired effects. The improved performance is achieved through a combination of electrode geometry, placement of the stages with respect to each other, and voltage pattern applied to the electrodes.

The corona electrodes and collecting electrodes are positioned parallel to each other extending between respective planes perpendicular to an airflow direction. All electrodes of neighboring stages are parallel to each other, with all the electrodes of the same kind (i.e., corona discharge electrodes or collecting electrodes) placed in the same parallel planes that are orthogonal to the planes where electrodes of the same kind or electrodes edges are located. The stages are spaced to avoid or minimize any corona discharge activity between the electrodes of neighboring stages. The experimental studies were conducted to determine the minimum possible distance between the neighboring stages. The distance between the corona discharge wire of one stage and the closest part of the neighboring stage should be a factor of 1.2 to 2.0 larger than the characteristic distance of the single stage a_n. Assuming voltage V_1 applied to

the corona electrode and voltage V_2 to the closest accelerating electrode of the same stage, the characteristic distance is defined here as

$$a_n = \left| \frac{V_1 - V_2}{E_n} \right|, \tag{1}$$

where E_n is the onset electric field intensity in the vicinity of the corona electrode for a given geometry of the accelerating stage.

Finally, voltages applied to neighboring stages should be synchronized and syn-phased. That is, a.c. components of the voltages applied to the electrodes of neighboring stages should rise and fall simultaneously and have substantially the same waveform and magnitude and/or amplitude. Operating in such a synchronous manner between stages, electrical potential differences between neighboring electrodes of adjacent EFA components remains constant and any resultant stray current from one electrode to another is minimized or completely avoided. Synchronization may be implemented by different means, but is accomplished most easily by powering neighboring EFA components with respective synchronous and syn-phased voltages from corresponding power supplies, or with power supplies synchronized to provide similar amplitude a.c. components of the respective applied voltages. This may be achieved with the same power supply connected to neighboring EFA components or with different, preferably matched power supplies that produce synchronous and syn-phased a.c. component of the applied voltage.

B. Energy density

The electric field energy is converted into a kinetic energy of moving air through collisions of ions with the air molecules. Naturally, higher velocities of air at the device outlet can be achieved by increasing the ion density. The larger number of ions can be generated by placing a multiple corona electrodes close to one another.

The energy could also be increased by increasing the electric field in the space between the electrodes. However, the power available from a single corona electrode is limited by air breakdown voltage. The range between the corona inception and the air breakdown is quite narrow, for any geometry.

The overall conclusion is that in order to increase the velocity of air, the electrode density should be increased. A straightforward way to achieve that is to stack the electrodes above each other, in a direction perpendicular to the air flow. However, doing so would lead to reduced electric field intensity near the corona wire. In the limit, an array of neighboring corona wires acts just like a plane electrode, not suitable for creating an inhomogeneous electric field. The solution to this problem lies in “screening” or shielding the corona electrodes from each other [27].

The corona electrodes can be placed close to each other and yet maintain the corona discharge if they are electrically shielded from each other. The shield-

ing effect can be achieved by designing geometry and excitation pattern for shielding electrodes in such a way that they still produce non-homogeneous electric field needed to generate a corona discharge. These electrodes must be placed between adjacent corona electrodes and, thus, across the intended direction of flow for the fluid molecules. This design feature leads to the third element of discussion, distribution of electric fields and design of electrode shapes most suitable for producing the air flow in the desired direction.

C. Efficiency of energy conversion

In order to cause ions to create fluid flow, either the exciting electrode must be asymmetrically located between the adjacent corona electrodes or there must be an accelerating electrode. Such an accelerating electrode is an attracting electrode placed downstream from the corona electrodes in order to cause the ions to move in the intended direction. The electric polarity of the attracting electrode is opposite to that of the corona electrode. The effect of electric field distribution on the efficiency of energy conversion has been previously studied in [28], however, at that time, the approach was focused strictly on electric fields and did not take into account the effects of fluid dynamics.

Although the concept of electrode placement and energization is relatively easy to conceive, the practical solution is not obvious, since the design space is very large. The reasoning for initial design is described above. Theoretical modeling and numerical simulations become especially important for the iterative design process of individual EFA stages. The next section presents our approach to multi-physics modeling of EFAs.

III. NUMERICAL MODELING

A. Governing equations

Electrohydrodynamic flow induced by corona discharge is described by the following equations. The electric potential V is governed by the Poisson's equation

$$\nabla^2 V = -\frac{q}{\varepsilon_0}, \tag{2}$$

where q is the space charge density and ε_0 is the dielectric permittivity of free space. The electric potential is defined from electric field intensity $\mathbf{E}$ as

$$\mathbf{E} = -\nabla V\,. \tag{3}$$

Electric current in the drifting zone is a combination of three effects: conduction (motion of ions under electric field relative to entire airflow), convection (transport of charges with airflow), and diffusion. Therefore, current density $\mathbf{J}$ is given by

$$\mathbf{J} = \mu_{\mathrm{E}} \mathbf{E} q + \mathbf{U} q - D \nabla q \,, \tag{4}$$

where μ_{E} is the air ions mobility in an electric field, $\mathbf{U}$ is velocity vector of airflow, and D is the diffusivity coefficient of ions. Current continuity condition gives equation for current density

$$\nabla \bullet \mathbf{J} = 0 \,. \tag{5}$$

Hydrodynamic part of the problem is described by Navier-Stokes equations and continuity equation for steady state incompressible air flow

$$\rho \mathbf{U} \bullet \nabla \mathbf{U} = -\nabla p + \mu \nabla^2 \mathbf{U} - q \nabla V \,, \tag{6}$$

$$\nabla \bullet \mathbf{U} = 0 \,, \tag{7}$$

where ρ is the air density, p is the air pressure, and μ is the air dynamic viscosity.

In addition, if electrodes have finite conductivity σ, then electric potential distribution inside them is governed by current continuity equation and Ohm's law

$$\nabla \bullet \mathbf{J}_{\mathrm{S}} = 0 \,, \tag{8}$$

$$\mathbf{J}_{\mathrm{S}} = -\sigma \nabla V_{\mathrm{S}} \,, \tag{9}$$

where $\mathbf{J}_{\mathrm{S}}$ and V_{S} are current and electric potential in solid respectively.

System of equations (2), (5), (6), (7), and (8) is subject to appropriate boundary conditions described below for the model studied in this paper.

B. Studied model and boundary conditions

In this paper we present some typical results of numerical simulations for the model consisting of an array of identical patterns. Cross section view of one pattern is shown in Fig. 1. It consists of a thin wire placed between two collecting electrodes inserted into flat conductive plates forming a short channel. All patterns are placed along a line perpendicular to the surface of conductive plates. Computational domain used for numerical simulations is denoted by the dashed line in Fig. 1. Only one half of the channel is needed for computations due to the symmetry of the problem.

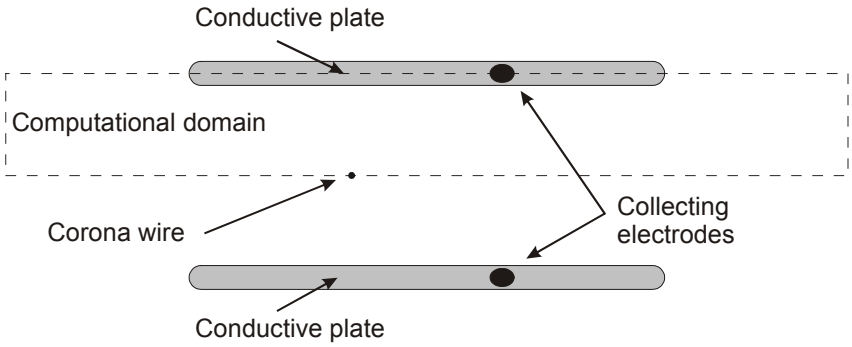

Fig. 1. Schematics of the studied model: thin wire is placed between two collecting electrodes inserted into conductive plates. Computational domain is shown by dashed line.

Boundary conditions for electric potential are straightforward. On the wire surface and surfaces of collecting electrodes we have prescribed voltage V_{W} and V_{C}, respectively. Symmetry conditions are used on top and bottom boundaries. At the inlet/outlet boundary electric potential is set to the value obtained from the assumption that electric potential decreases inversely proportional to the distance from the wire, i.e. $V_{\mathrm{W}} R_{\mathrm{W}} / d$, where d is the distance between wire and inlet/outlet boundary and R_{W} is the wire radius. This assumption is reasonable because inlet and outlet boundaries are far enough from the corona wire (real computational domain is longer that shown in Fig. 1). On the surface of conductive plate, continuity condition is used for electric potential in drifting zone and in solid.

Boundary conditions for the space charge need additional discussion. In the close vicinity of the corona electrode there exists an ionization zone where both positive and negative ions are present. When the radius of corona electrode is much larger than the distance between corona and collecting electrodes, the ionization zone forms a uniform sheath over the wire surface. In corona discharge modeling, the thickness of the ionization zone is usually ignored completely. This assumption has little effect on voltage-current solution, but it can considerably overestimate electrohydrodynamic pressure [29]. We take into account thickness of ionization zone, as it does not present any difficulties in the case of corona wire. For the positive corona, the electric field strength E_{W} at surface of a smooth corona wire of radius R_{W} is given by empirical Peek's formula for air at standard conditions [30]

$$E_{\mathrm{W}} = E_0 \left(1 + 2.62 \cdot 10^{-2} / \sqrt{R_{\mathrm{W}}}\right), \tag{10}$$

where wire radius R_{W} is measured in m and $E_0 = 3.23 \cdot 10^6$ V/m is the breakdown (ionizing) electric strength in air. In contrast with the drifting zone, the space charge density is negligible in the ionization zone. Thus, assuming that the wire radius is much smaller than the distance between corona electrode and collecting electrodes, the electric potential and electric field intensity decrease inside the ionization zone as

$$V = V_{\mathrm{W}} - E_{\mathrm{W}} R_{\mathrm{W}} \ln \frac{r}{R_{\mathrm{W}}}, \tag{11}$$

$$E = E_{\mathrm{W}} \frac{R_{\mathrm{W}}}{r}. \tag{12}$$

At the boundary between ionization and drifting zones the electric field strength is equal to breakdown electric field strength E_0. Using above expressions one can easily find external radius of ionization zone, which is solely a function of R_{W}:

$$R_0 = R_{\mathrm{W}} E_{\mathrm{W}} / E_0 = R_{\mathrm{W}} \left(1 + 2.62 \cdot 10^{-2} / \sqrt{R_{\mathrm{W}}}\right). \tag{13}$$

The voltage drop in ionization zone can be found by integrating electric field strength from R_{W} to R_0. As a result, the voltage on the external boundary of the ionization zone is given by

$$V_0 = V_{\mathrm{W}} - E_{\mathrm{W}} R_{\mathrm{W}} \ln \frac{E_{\mathrm{W}}}{E_0}. \tag{14}$$

Therefore, Poisson's equation for electric potential is to be solved only inside the drifting zone with the prescribed voltage V_0 on the external boundary of the ionization zone.

For charge transport equation, also to be solved only inside the drifting zone, we impose zero diffusive flux condition, $dq / dn = 0$, on all boundaries except for the external surface of the ionization zone. The validity of this assumption is justified by the fact that the outflow boundary conditions for charge density are necessary only when the diffusion term is present in (5), which has negligible effect on charge density distribution in corona current modeling [31,32]. At the external surface of ionization zone we use Kaptsov's

assumption [33], which does not provide direct description of charge but specifies the electric field strength: $E = E_0$ at $r = R_0$.

For the electric potential equation inside the conductive plate, we use symmetry condition on top boundary and continuity condition for the electric potential and current on boundary between plate and drifting zone.

Boundary conditions for air flow are quite straightforward: no slip conditions on all solid surfaces (wire and both conductive plates) $u = v = 0$; symmetry conditions on other top and bottom boundaries $du/dn = v = 0$; and inflow and outflow boundary conditions on the inlet and outlet boundaries, respectively.

C. Results of numerical simulations

Numerical simulations were carried out using FEMLAB software, a commercial software package that performs equation-based multiphysics modeling for different physical processes by applying the finite element method to a system of partial differential equations. Typical results of simulations are shown in Fig. 2 through Fig. 4.

Specifically, Fig. 2 shows the electric potential distribution and streamlines of electric current for the described above simulation setup. Space charge density distribution and air velocity field are shown in Fig. 3 and Fig. 4, respectively. The distance between the center of the wire and the center of the collecting electrode is 5 mm in the horizontal direction, and the gap between channel walls is 6 mm. The thickness of channel walls is 0.8 mm and their conductivity is $5 \cdot 10^{-7}$ $(\text{Ohm} \cdot \text{m})^{-1}$. The cross-section of the collecting electrode is an ellipse with the axes of 0.4 mm and 0.3 mm. The wire radius is 0.05 mm. High voltage difference applied between the wire and the collecting electrodes is 7.5 kV. The calculated average air velocity at the outlet of the channel is 5.6 m/s.

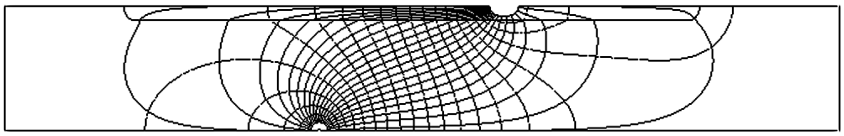

Fig. 2. Electric potential distribution and streamlines of electrical current for model described in the text and shown in Fig. 1.

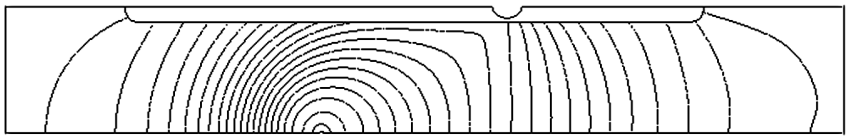

Fig. 3. Space charge density distribution in the drifting zone for the conditions of Fig. 2.

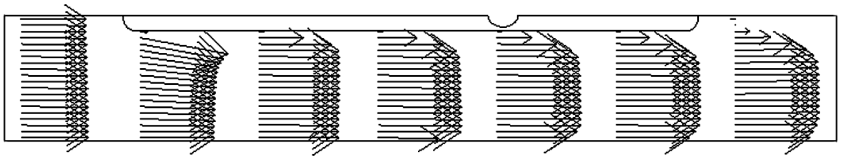

Fig. 4. Air velocity field for the conditions of Fig. 2.

IV. Experimental Results

The conceptual improvements, theoretical studies, and iterative design approach resulted in the highest air velocity at the EFA outlet reported in technical literature up to date. Fig. 5 shows the air velocity measured at the cross section of the EFA built to generate very fast air flow at the outlet. The EFA comprised 12 accelerating stages, stacked sequentially. The average value of 7.5 m/s (about 1500 f/min) was achieved in the entire central area of the cross-section. Notice that a similar cross-section for a rotary fan would have a dip in the very middle of the cross-section, because of the motor placed in the center.

The relationship between the number of stages and the resulting air velocity is not linear. Fig. 6 show the experimental data for 4, 8 and 12 EFA arrays stacked sequentially together. For the small number of arrays, the ratio of the air velocities is approximately equal to the square of the ratio of the number of stages.

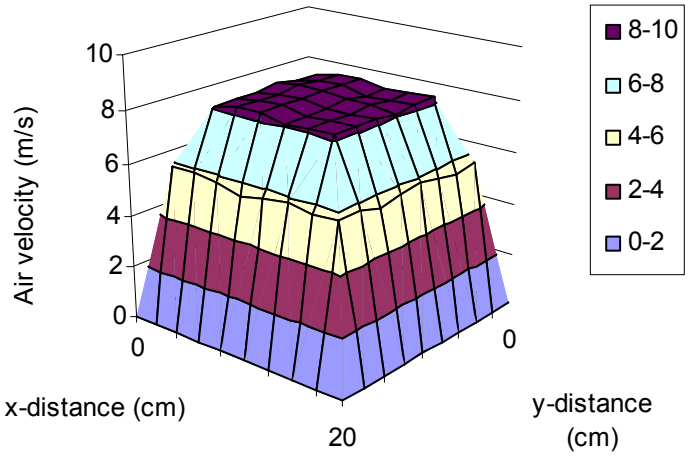

Fig. 5. Measured air velocity in the cross-section of a 12-stage optimized EFA.

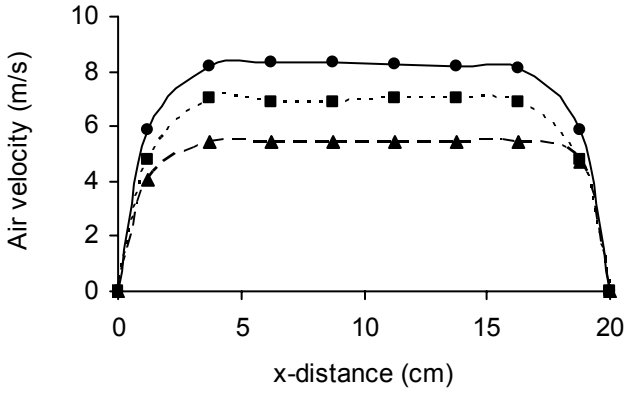

Fig. 6. Measured air velocity along the centerline of EFA outlet for different numbers of stages: 12 (circles), 8 (squares), and 4 (triangles). The lines connecting symbols are only guides to the eye.

V. Acknowledgements

This project was partially supported by the Washington Technology Center grant RTD 05 UW MC01.

REFERENCES

[1] J. E. Bryan and J. Seyedyagoobi, "Experimental-Study of Ion-Drag Pumping Using Various Working Fluids," *IEEE Transactions on Electrical Insulation*, vol. 26, no. 4, pp. 647-655, Aug. 1991.

[2] C. A. Belhadj, A. S. Shwehdi, and A. S. Farag, "Corona Wind Velocity: Parametric Approach," 1998, pp. 489-492.

[3] G. M. Colver and S. El-Khabiry, "Modeling of DC Corona Discharge Along an Electrically Conductive Flat Plate With Gas Flow," *IEEE Transactions on Industry Applications*, vol. 35, no. 2, pp. 387-394, Mar. 1999.

[4] L. Leger, E. Moreau, and G. G. Touchard, "Effect of a DC Corona Electrical Discharge on the Airflow Along a Flat Plate," *IEEE Transactions on Industry Applications*, vol. 38, no. 6, pp. 1478-1485, Nov. 2002.

[5] J. R. Roth, "Aerodynamic Flow Acceleration Using Paraelectric and Peristaltic Electrohydrodynamic Effects of a One Atmosphere Uniform Glow Discharge Plasma," *Physics of Plasmas*, vol. 10, no. 5, pp. 2117-2126, May 2003.

[6] J. A. Cross, "Electrostatically Assisted Heat Transfer," *International Electrostatics Conference*, 1975, pp. 191-199.

[7] J. Mathew and F. C. Lai, "Enhanced Heat Transfer in a Horizontal Channel With Double Electrodes," *IEEE Industry Applications Conference*, vol. 2, 1995, pp. 1472-1479.

[8] M. E. Franke and L. E. Hogue, "Electrostatic Cooling of A Horizontal Cylinder," *Journal of Heat Transfer-Transactions of the Asme*, vol. 113, no. 3, pp. 544-548, Aug. 1991.

[9] Takimoto, A., Tada, Y., and Hayashi, K., "Convective Heat-Transfer Enhancement by a Corona Discharge," Sumitomo Electric Industry Co., Ltd., 1991.

[10] D. Schilitz, S. Garimella, and T. Fisher, "Numerical Simulation of Microscale Ion Driven Air Flow," *ASME IMECE*, 2003.

[11] H. Kalman and E. Sher, "Enhancement of Heat Transfer by Means of a Corona Wind Created by a Wire Electrode and Confined Wings Assembly," *Applied Thermal Engineering*, vol. 21, no. 3, pp. 265-282, Feb. 2001.

[12] F. Yang, N. E. Jewell-Larsen, D. L. Brown, D. A. Parker, K. A. Pendergrass, I. A. Krichtafovitch, and A. V. Mamishev, "Corona Driven Air Propulsion for Cooling of Electronics," *International Symposium on High Voltage Engineering*, 2003.

[13] A. Shooshtari, M. M. Ohadi, and F. H. R. Franca, "Experimental and Numerical Analysis of Electrohydrodynamic Enhancement of Heat Transfer in Air Laminar Channel Flow," *19th IEEE SEMI-THERM Symposium*, San Jose, CA, 3-11-2003.

[14] F. Bastien, "Acoustics and Gas Discharges: Applications to Loudspeakers," *J.Phys.D: Appl.Phys.*, vol. 8, no. 20, pp. 1547-1557, Dec. 1987.

[15] S. A. Hoenig, "New Technology for Detection and Removal of Surface Contamination Involving Particulates or Water/Organic Materials," *42nd Annual Frequency Control Symposium*, 1988, pp. 189-201.

[16] H. Uchiyama and M. Jyumonji, "Field Experiments of an Electrostatic Fog-Liquefier," *Proc. ESA-IEJ Joint Symp. Electrostatics*, 1994, pp. 97-104.

[17] S. A. Hoenig, "New Applications of Electrostatic Technology to Control of Dust, Fumes, Smokes, and Aerosols," vol. IA-17, 1981, pp. 386-391.

[18] G. M. Colver and S. El-Khabiry, "Modeling of DC Corona Discharge Along an Electrically Conductive Flat Plate With Gas Flow," *IEEE Transactions on Industry Applications*, vol. 35, no. 2, pp. 387-394, Mar. 1999.

[19] L. Leger, E. Moreau, and G. G. Touchard, "Effect of a DC Corona Electrical Discharge on the Airflow Along a Flat Plate," *IEEE Transactions on Industry Applications*, vol. 38, no. 6, pp. 1478-1485, Nov. 2002.

[20] F. Yang, "*Corona-driven air propulsion for cooling of microelectronics*," Masters Thesis, Department of Electrical Engineering, University of Washington, Seattle, WA, 2002.

[21] K. Adamiak, "Adaptive Approach to Finite Element Modeling of Corona Fields," *IEEE Transactions on Industry Applications*, vol. 30, no. 2, pp. 387-393, Mar. 1994.

[22] J. E. Bryan and J. Seyed-Yagoobi, "Analysis of 2-Dimensional Flow Field Generated by a 1-Electrode-Pair Ion-Drag Pump," *IEEE Transactions on Dielectrics and Electrical Insulation*, vol. 1, no. 3, pp. 459-466, June 1994.

[23] G. M. Colver and S. El-Khabiry, "Modeling of DC Corona Discharge Along an Electrically Conductive Flat Plate With Gas Flow," *IEEE Transactions on Industry Applications*, vol. 35, no. 2, pp. 387-394, Mar. 1999.

[24] K. Sakai, S. Tsuru, D. L. Abella, and M. Hara, "Conducting Particle Motion and Particle-Initiated Breakdown in Dc Electric Field Between Diverging Conducting Plates in Atmospheric Air," *IEEE Transactions on Dielectrics and Electrical Insulation*, vol. 6, no. 1, pp. 122-130, Feb. 1999.

[25] E. J. Shaughnessy and G. S. Solomon, "Electrohydrodynamic Pressure of the Point-To-Plane Corona Discharge," *Aerosol Science and Technology*, vol. 14, no. 2, pp. 193-200, 1991.

[26] I. A. Krichtafovitch and V. L. Gorobets, "Electrostatic fluid accelerator for and a method of controlling fluid flow," US Patent No.6,727,657, Apr. 2004.

[27] I. A. Krichtafovitch and R. L. Fuhriman, "Electrostatic fluid accelerator," USA Patent No.6,504,308, Jan. 2003.

[28] N. E. Jewell-Larsen, D. A. Parker, I. A. Krichtafovitch, and A. V. Mamishev, "Numerical Simulation and Optimization of Electrostatic Air Pumps," *Annual Report Conference on Electrical Insulation and Dielectric Phenomena*, 2004, pp. 106-109.

[29] Jullian, M., "FECAW wire cylinder corona tutorial, in SI units. Electrostatics, space charge and fluid mechanics simulation," 2004.

[30] F. W. Peek, *Dielectric Phenomena in High Voltage Engineering,* New York:McGraw-Hill, 1929.

[31] J. Q. Feng, "Application of Galerkin Finite-Element Method With Newton Iterations in Computing Steady-State Solutions of Unipolar Charge Currents in Corona Devices," *Journal of Computational Physics*, vol. 151, pp. 969-989, 1999.

[32] J. Q. Feng, "Electrohydrodynamic Flow Associated With Unipolar Charge Current Due to Corona Discharge From a Wire Enclosed in a Rectangular Shield," *Journal of Applied Physics*, vol. 86, no. 5, pp. 2412-2418, 1999.

[33] N. A. Kaptsov, *Elektricheskie Yavleniya v Gazakh i Vakuume,* Moscow, OGIZ, 1947.